Cross sections for electron capture and loss. I. H^+ and H^- impact on H and H_2

M. W. Gealy* and B. Van Zyl
Department of Physics, University of Denver, Denver, Colorado 80208
(Received 27 April 1987)

The electron-capture cross sections for H^+ impact on H and H_2 and the electron-loss cross sections for H^- impact on H and H_2 have been measured for projectile energies between 2.0 and 0.063 keV. Relative cross-section values for all these reactions were measured directly, and placed on an absolute scale by adopting a standard value of 6.95×10^{-16} cm^2 for the electron-capture cross section for $H^+ + H_2$ collisions at 2.0-keV H^+ energy. A crossed-beam technique was used, and the reaction-product H atoms were measured by a secondary-electron-emission detector. The techniques used to make the measurements are described, and the results are compared with other experimental and theoretical data.

I. INTRODUCTION

The electron-capture cross sections (σ_{10}) and the electron-loss cross sections (σ_{-10}) have been measured, respectively, for H^+ and H^- impact on H and H_2 targets. The projectile-energy range covered was from 2.0 to 0.063 keV. The cross sections for electron capture (σ_{0-1}) and electron loss (σ_{01}) for H-atom impact on H and H_2 targets were also measured for similar projectile energies and are reported in the following paper[1] (henceforth referred to as paper II). All of these reactions are theoretically the simplest that can occur for their respective types, and data for these processes find numerous applications ranging from problems in theoretical astrophysics to understanding thermonuclear-fusion devices.

Ranking as one of nature's most fundamental processes, the capture of electrons by H^+ incident on H has been the subject of many theoretical technique-evaluation studies over the years. The failure at low H^+ energies of simple first Born calculations as made by Jackson and Schiff,[2] for example, has led to various theoretical refinements, such as the perturbed-stationary-state treatment applied by Dalgarno and Yadav[3] and, more recently, to such detailed close-coupling calculations as those of Shakeshaft,[4] to cite but two.

From an experimental viewpoint, the pioneering efforts of Fite and colleagues[5] were followed by, among others, McClure,[6] and more recently, the elegant low-H^+-energy, merged-beam studies of Newman *et al.*[7] For H^+ energies below 10 keV, the range of interest here, the data of McClure[6] down to 2-keV H^+ energy, and those of Newman *et al.*[7] up to about 0.3-keV H^+ energy, are in excellent agreement with the theoretical prediction of Dalgarno and Yadav.[3]

For $H^- + H$ collisions, the σ_{-10} data of Geddes *et al.*[8] and of Hummer *et al.*[9] are well within mutual uncertainties for H^- energies between 1 and 10 keV. The Hummer *et al.*[9] data, which separate σ_{-10} into its $H^- + H \rightarrow H + H + e^-$ electron-stripping and $H^- + H \rightarrow H + H^-$ electron-capture components down to near 0.4-keV H^- energy, are in close agreement (for the electron-capture component) with the theory of Dalgarno and McDowell[10] down to 0.04-keV H^- energy.

Why then did we undertake the present additional cross-section measurements? Our primary motivation was likewise to employ these relatively well-understood reactions as technique-evaluation standards. In paper II we present the results of similar studies for H + H collisions, for which no other data exist in this projectile-energy range. Our longer-range goals include the same measurements involving atomic-oxygen targets, for which much less data are available and, eventually, extension of the work to examine collisional-excitation processes. Thus, the basic measurement techniques, to be described here in detail for future reference, have been rehearsed on these simpler and well-quantified reactions.

We did not, however, make these studies for this reason only. In our opinion, these reactions are of sufficient basic and applied importance to warrant periodic study and review as new measurement technologies are developed. All fields of research benefit from having numerous measurements of their most standard and fundamental processes, and we would include these reactions in this category.

Furthermore, for the case of H_2 targets, the σ_{10} results of Stedeford and Hasted,[11] Gustafson and Lindholm,[12] Cramer,[13] and Koopman[14] exhibit substantial scatter (about a factor of 2) for H^+ energies below 1 keV. The σ_{-10} data reported by Geddes *et al.*,[8] Hasted and Smith,[15] Muschlitz *et al.*,[16] Risley and Geballe,[17] and Huq *et al.*[18] also show significant differences at lower H^- energies, so that another independent study of these reactions is warranted.

II. EXPERIMENTAL APPARATUS

The basic apparatus used to generate the fast-ion beams has been described elsewhere[19] and will not be reviewed here in detail. Essentially, ions were extracted from a duoplasmatron source, mass analyzed, and brought to their desired energy and trajectory by a three-component electrostatic lens assembly containing ion-steering electrodes. They were then electrostatically deflected through an angle of about 9°, which pointed

them towards their intersection with the target-beam axis about 12.7 cm downstream.

Located along this ion-beam path, about 3.3 cm beyond the 9° bend, was an auxiliary ion collector (whose primary purpose was to remove ions from the beam trajectory during the H-atom-beam work described in paper II). Here, ions could be electrostatically diverted into a guarded Faraday cup with 50% duty cycle, to monitor their intensity for comparison with that at other downstream locations. This allowed assessment of various beam-alignment, beam-focus, and at the lower ion energies, beam-spreading effects, needed for proper analysis of the measurement results.

The target-beam source, located in a separate differentially pumped vacuum chamber, was a tubular molecular-dissociation furnace from whose open end emerged the target-beam particles. The back end of this tungsten furnance tube (about 7.6 cm long and 0.26 cm in diameter) was silver soldered to a water-cooled copper reservoir serving as a constant-flow (and pressure-monitored) source of H_2 for the furnace. The front 3.5 cm of the tube could be heated up to about 2400 K by electron-impact bombardment from eight thoria-coated iridium filaments which were suspended as loops around the furnace tube (in a horseshoe shape) from two large water-cooled conductors. This source, shown in a top cross-sectional view in Fig. 1, and its operational characteristics (such as the dissociation fraction versus temperature of the emergent particles, and their collimated angular-flow distributions from the furnace tube[20]) has been described elsewhere in detail.[21,22]

The differential-pumping and beam-skimming apertures were rectangular in shape (with rounded corners). Their long dimensions were in the horizontal plane, to maximize the interaction length (about 1 cm) for the fast ions traversing the target beam. Their vertical dimensions were kept small (the first only about 0.15 cm), to minimize the flow of gas from the furnace chamber into the interaction region and main vacuum tank (called the scattering chamber). To further reduce this gas load in the scattering chamber,[20] the target-beam particles, after traversing the interaction region, entered another differentially pumped chamber. (A quadrupole mass spectrometer could also be situated here to perform dissociation-fraction measurements on the target-beam particles.) With H_2 gas in the reservoir at 0.1 Torr pressure, the pressure in the furnace chamber was about 5×10^{-5} Torr, in the scattering chamber about 5×10^{-7} Torr, and in the quadrupole chamber about 1×10^{-7} Torr.

A schematic view (again from the top) of the interaction region and fast-particle detectors is shown in Fig. 2. Just prior to the interaction region, the fast ions could be (electrostatically) diverted from reaching the interaction region by the ion deflectors (whose purpose will be discussed in Sec. III). After traversing the interaction region, the primary-beam ions were deflected by the charge-state-separator electrodes to their respective Faraday-cup collectors, while the reaction-product H atoms impinged on a copper surface where their secondary-electron yield could be monitored.

The secondary-electron-emission coefficient (γ^-) for such a copper surface, or more importantly for the present work, its relative dependence on incident H-atom energy, has been previously measured in this laboratory.[23] It was also carefully remeasured here on numerous occasions during these studies. An analysis of all such data indicated that the value of γ^- as a function of H-atom energy relative to its value at 2-keV H-atom energy was reproducible to within ±6.8% at the 90% confidence level (CL), which was taken here to be its (relative) uncertainty for these measurements. (We attempted to assess all such uncertainties at the 90% CL or higher.)

The electrodes containing aperture A (0.5 cm diameter), aperture B (0.4 cm diameter), and the apertures fronting all collectors (1.0 cm diameter) were electrically isolated to allow measurement of arriving ion currents, or leaving secondary-electron currents from H-atom impact. Such measurements were used primarily for various beam-alignment and beam-profile studies, but could also be used to assess the magnitude of angular scattering of the fast-beam particles in the interaction region. To further examine such effects, the entire collector assembly could be rotated (in the horizontal plane) about an axis near the center of the charge-state separators.

The magnitudes of the primary ion-beam currents were typically between 0.2 and 1.5×10^{-6} A. Secondary-electron-yield currents ranged between about 0.01 and 2.5×10^{-11} A. Because the cross-section mea-

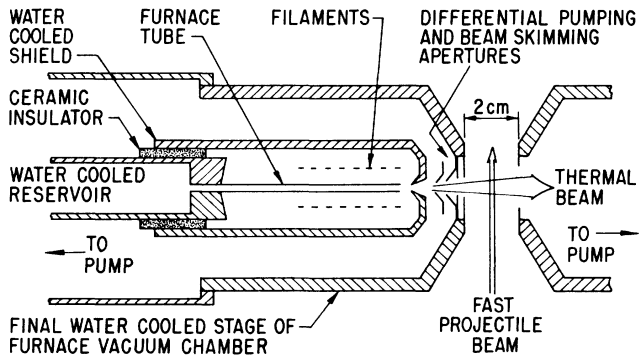

FIG. 1. Top view of furnace assembly for target-beam production.

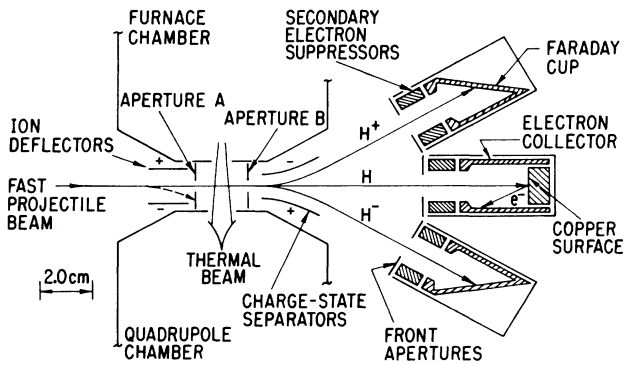

FIG. 2. Top view of interaction region and particle collectors.

surements reported here were placed on an absolute scale by normalizing to other data, there was no need to calibrate absolutely the electrometers used for these current measurements.

III. MEASUREMENT TECHNIQUES AND DIAGNOSTICS

In an ideal experiment, the ratio of the cross section σ_a for a projectile-neutralizing reaction (at fixed projectile energy) involving an atomic target to the same cross section σ_m for a molecular target can be obtained quite simply using the apparatus described above. The normalized H-atom signal (secondary-electron yield per unit primary-ion intensity) from such ion-target collisions with the furnace at room temperature (T_0) can be written as

$$S_t(T_0)=\gamma^- L_t \sigma_m N_{\rm tm}(T_0)\ , \tag{1}$$

and at elevated furnace temperature (T) as

$$S_t(T)=\gamma^- L_t[\sigma_m N_{\rm tm}(T)+\sigma_a N_{\rm ta}(T)]\ . \tag{2}$$

Here, γ^- is again the secondary-electron-emission coefficient for the H-atom detector, and L_t is the length of interaction path for the fast ions crossing the target beam. $N_{\rm tm}(T_0)$, $N_{\rm tm}(T)$, and $N_{\rm ta}(T)$ are the effective densities of target molecules and atoms in the beam from the furnace at the temperatures indicated. We call these effective densities because they include the overlap integrals of the spatial distributions of the intersecting beams.

The desired σ_a/σ_m can be found from Eqs. (1) and (2) to be

$$\frac{\sigma_a}{\sigma_m}=\left[\frac{N_{\rm ta}(T)}{N_{\rm tm}(T_0)}\right]^{-1}\left[\frac{S_t(T)}{S_t(T_0)}-\frac{N_{\rm tm}(T)}{N_{\rm tm}(T_0)}\right]\ . \tag{3}$$

As can be seen, only normalized-signal and effective-target-density ratios enter this expression, which ratios are much easier to measure than the absolute values of these individual parameters.

The effective target densities $N_{\rm tm}(T)$ and $N_{\rm ta}(T)$ relative to $N_{\rm tm}(T_0)$ were calculated. The actual relative densities for on-axis particle flow from the furnace tube were measured,[21] and are shown by the data points and solid-line curves in Fig. 3. These data were convoluted with the angular distribution of this particle flow[21] and the geometrical restrictions imposed by the differential-pumping and beam-skimming apertures shown in Fig. 1, to find the spatial profile of the target beam in the interaction region as a function of furnace temperature. The spatial profiles of the fast projectile beams had been measured previously,[24] but were confirmed here by sweeping the beam ions across various aperture edges along the beam path.

Using these data, the overlap integrals of the spatial-distribution profiles of the intersecting beams were computed numerically as functions of furnace temperature and ion energy. Examples of the resulting ratios $N_{\rm tm}(T)/N_{\rm tm}(T_0)$ and $N_{\rm ta}(T)/N_{\rm tm}(T_0)$ appearing in Eq. (3) are shown by the dashed-line curves in Fig. 3 for an

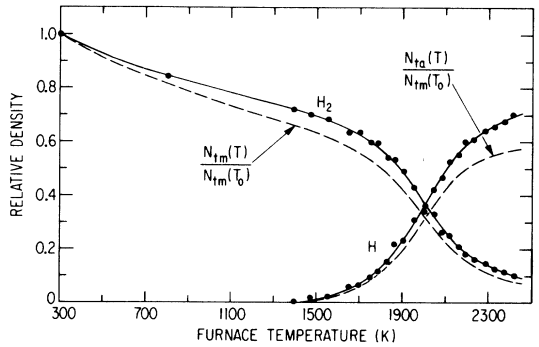

FIG. 3. Relative densities of H and H_2 in target beam vs furnace temperature.

H^+ energy of 0.5 keV. As can be seen, these effective-target-density ratios fall increasingly below the measured on-axis density ratios at the higher furnace temperatures. This largely reflects the increase in the target-beam collimation at higher furnace temperatures,[21] so that the target-particle densities become smaller at positions along the ion path which are somewhat off the furnace-beam axis. The effective-target-density ratios computed in this way were judged to be uncertain by $\pm 8.7\%$ (again at the 90% CL) at $T=2400$ K.

Similar studies were made to find how $N_{\rm tm}(T_0)$ varied as a function of ion energy relative to its value at 2 keV ion energy. This information was needed to determine the projectile-energy dependences of σ_{10} and σ_{-10} for H_2 targets. The uncertainties in these relative $N_{\rm tm}(T_0)$ values were found to increase with decreasing ion energy, but did not exceed $\pm 6.3\%$.

An analysis of the data obtained here would thus not have been difficult if the ideal experiment described above could have been performed. In practice, however, we had to contend with three other sources of H-atom signal, which are now discussed.

The first of these was production of H atoms by collisions of the projectile ions with the background particles present in the scattering chamber. While the density of these particles was only a few percent of that in the target beam, such H-atom production could occur anywhere along the 14.6-cm ion path between the 9° beam bend discussed in Sec. II and the charge-state separators shown in Fig. 2. In addition, σ_{10}, in particular, was found for these background species (mostly H_2O and hydrocarbons, according to quadrupole mass spectra) to be several orders of magnitude larger than that for H_2 at the lower H^+ energies.[25] It was thus always necessary to include measurements made with the target beam off, to determine and subtract out these background-gas signals. (We assume this has been done for discussion of all other signals below.)

Another source of H-atom signal was due to collisions of the beam ions with the residual hydrogen present in the scattering chamber whenever H_2 was introduced into the furnace. This gas density was also much smaller (about an order of magnitude) than that in the target beam, but detectable H atoms could again be produced

anywhere along the 14.6-cm ion path noted above. This was the reason for including the ion deflectors shown in Fig. 2. With these deflectors on, only H atoms produced upstream from the deflectors along a 10.0-cm ion path could be observed. Thus, multiplying the deflectors-on signal by the ion-path ratio $14.6/10.0=1.46$ allowed this source of signal to be evaluated for the deflectors-off measurements.[26]

Of course, use of this ion-path ratio in this way assumes that none of these collisionally produced H atoms were angularly scattered beyond detectable limits. This was expected to be the case at the higher projectile energies and, in fact, was verified experimentally[27] at 2 keV ion energy, but was not found to be true at the lower projectile energies, as will be discussed below.

The final source of extra H-atom signal is closely related to that discussed above. The residual hydrogen in the scattering chamber resulted from the net flow of gas from the higher-pressure furnace chamber into the scattering chamber, manifesting itself as a "jet" of particles streaming directly into the interaction region from the differential-pumping and beam-skimming apertures.[28]

To evaluate the average particle density in this jet (along the 2-cm ion path between apertures A and B in Fig. 2), provision was made to introduce gas into the furnace chamber other than through the furnace tube itself. We called this the bypass mode of operation. By adjusting this gas flow until the same residual-hydrogen pressure in the scattering chamber was obtained as with gas in the furnace tube, the flow of gas in the jet could be duplicated. (Remember that the particles in the furnace-produced target beam itself all flow directly into the very-low-pressure quadrupole chamber and cannot, therefore, contribute significantly to this jet.)

Under this condition, we can formalize the above discussion by defining the following measurable H-atom signals.

(i) Gas in furnace mode, deflectors off,

$$S_F(T_0)=\gamma^{-}\sigma_m[L_rN_r(T_0)+L_jN_j(T_0)]+S_t(T_0)\ ; \tag{4}$$

(ii) gas in furnace mode, deflectors on,

$$S_f(T_0)=\gamma^{-}\sigma_m[l_rN_r(T_0)]\ ; \tag{5}$$

(iii) gas in bypass mode, deflectors off,

$$S_B(T_0)=\gamma^{-}\sigma_m[L_rN_r(T_0)+L_jN_j(T_0)]\ ; \tag{6}$$

(iv) gas in bypass made, deflectors on,

$$S_b(T_0)=\gamma^{-}\sigma_m[l_rN_r(T_0)]\ . \tag{7}$$

Here, $N_r(T_0)$ is the residual-hydrogen density in the scattering chamber, and L_r and l_r are the ion paths along which detectable H-atom signal can result from ion impact on this residual hydrogen for the deflectors off or on cases, respectively. $N_j(T_0)$ and L_j are the equivalent quantities for the jet. Note that the signals $S_f(T_0)$ and $S_b(T_0)$ are here the same, the consequence, of course, of equating the scattering-chamber pressure and therefore the density, $N_r(T_0)$, in the two modes of operation. For the same reason, the contributions to $S_F(T_0)$ and $S_B(T_0)$ from the jet are also the same.

The $S_t(T_0)$ in Eq. (4) is the signal of interest here resulting from ion interactions with the target-beam molecules, as defined by Eq. (1). This signal can now be determined directly from experimentally measurable quantities by

$$S_t(T_0)=S_F(T_0)-S_B(T_0)\ , \tag{8}$$

$$=S_F(T_0)-KS_f(T_0)\ , \tag{9}$$

where the parameter K in Eq. (9) is

$$K=\frac{S_B(T_0)}{S_b(T_0)}=\frac{S_B(T_0)}{S_t(T_0)}\ , \tag{10}$$

$$=\frac{L_r}{l_r}+\frac{L_jN_j(T_0)}{l_rN_r(T_0)}\ . \tag{11}$$

As can be seen, the parameter K contains the L_r/l_r ion-path ratio, plus a term which includes the jet quantities L_j and $N_j(T_0)$. Measurement of K via Eq. (10) gave $K=2.04\pm0.8\%$ at 2 keV projectile energy. Using this value in Eq. (11), together with the values of $L_r=14.6$ cm, $l_r=10.0$ cm, and $L_j=2.0$ cm discussed above, gives $N_j(T_0)/N_r(T_0)=2.90$. Thus, ignoring the density of hydrogen particles in this jet[28] would have caused serious error (and was essential for interpretation of the measurements reported in paper II).

Note, however, that the use of either Eqs. (8) or (9) to find $S_t(T_0)$ is not limited to the case we have been discussing, where at 2 keV projectile energies, all H atoms produced along L_r and l_r can be detected.[27] At lower projectile energies, we should expect an increasing fraction of these atoms to be angularly scattered beyond detectable limits, beginning with those produced well upstream from the ion deflectors. Thus, the "effective" ion paths L_r and l_r over which detectable atoms could be formed, should both decrease by the same amount, causing the value of K from Eq. (11) to increase with decreasing projectile energy.

As noted in Sec. II, currents to the apertures fronting the various collectors (see Fig. 2) could be measured, and the collector assembly itself could be rotated, to study the angular scattering of reaction-product H atoms formed in the interaction region. A number of such studies were made, but we found no evidence that less than 100% of these atoms were ever being collected (the H-atom signals recorded were always "flat-topped" over at least some range of collector-rotation angle), although such data for low-energy H^+ impact on H_2 were sufficiently scattered[25] to be rather inconclusive. However, the dependence of the parameter K on projectile energy provided an alternate method to examine this problem.

We show in Fig. 4 the projectile-energy dependences of the values of K measured here. Relative K values, normalized to unity at 2 keV projectile energy, are shown, so that we can include data obtained with both dc and ac beams, which exhibit different absolute values[26] of K. Note that, even for $H^+ + H_2$ collisions at 0.063 keV H^+ energy, the value of K for this reaction has only increased by a factor of about 2.5. These data

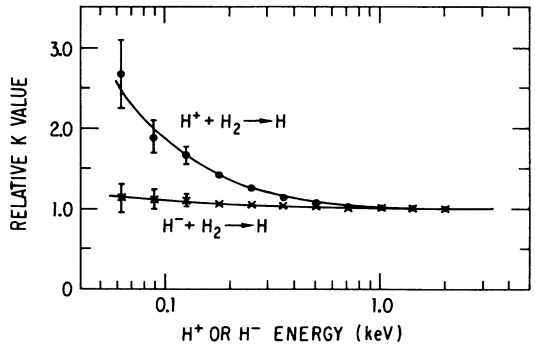

FIG. 4. Relative values of K vs primary-ion energy.

can be used via Eq. (11) to show that, even in this worst-case situation, we were still effectively collecting H atoms (from H^+ impact on residual H_2) produced more than 2.5 cm upstream from the ion deflectors. At this location, the solid angle for such H-atom collection was less than half of that available to H atoms produced in the interaction region (as defined by a 4° half-angle cone). We thus concluded that the loss of any H-atom signal from the reactions of interest was minimal.[29]

The data in Fig. 4 also indicate that significantly less angular scattering occurs for H-atom production by electron loss from H^- than occurs for the H^+ electron-capture process. This is intuitively pleasing, for the small electron affinity (about 0.75 eV) and the large electron radius (about $5.3a_0$) of H^- both contribute to the ease with which electron detachment can occur at large impact parameters, and thus without significant momentum transfer.

According to calculations such as have been made by Baskes,[30] very-low-energy H atoms (say, near $T=2400$ K) incident on a nickel surface should have a very small reflection probability per collision (only about 0.1). Similar small values were expected for the stainless steel and copper surfaces present in our system.[31]

Because the particles composing the jet and, eventually, the residual hydrogen in the scattering chamber, must have made an extreme minimum of two such wall collisions (many more, on average) before emerging from the furnace chamber, it was anticipated that virtually all these particles would be H_2, even at high furnace temperatures. Thus, the product H-atom signals associated with ion impact on the jet and residual hydrogen particles should be independent of furnace temperature. The only modifications needed to apply Eqs. (4)–(11) at higher furnance temperatures would then be to replace $S_F(T_0)$ by $S_F(T)$, and $S_t(T_0)$ by $S_t(T)$. It was, of course, necessary to experimentally verify this hypothesis, and we now present the results of one such study.

The available σ_{10} data discussed in Sec. I indicate that for 0.5-keV H^+ impact on H and H_2, the ratio $\sigma_a/\sigma_m \simeq 10$. We would thus expect that, after an initial small decrease with furnace temperature because of the initial H_2-target-beam-density decrease shown in Fig. 3, the (gas in tube, deflectors off) signal $S_F(T)$ would rapidly increase for $T > 1500$ K, in proportion to the increasing H-atom component of the target beam. The measured values of $S_F(T)$ are shown by the upper curve in Fig. 5(a), and confirm these expectations. Also shown in Fig. 5(a), however, are the measured (gas in tube, deflectors on) signals $S_f(T)$, which we predicted above would be independent of furnace temperature. While this appears to be true for $T < 1500$ K, it is clearly not true for $T > 1500$ K. We know of no possible explanation for these data, except that the residual hydrogen in the scattering chamber was partially dissociated.[32]

This finding was initially of serious concern. It was clear that an expression such as Eq. (8) could no longer be used to obtain $S_t(T)$, for the residual-hydrogen dissociation fractions were found to be different[22] for the normal and gas-bypass modes of operation. We soon realized, however, that $S_t(T)$ as given by Eq. (9) with (T_0) replaced by (T), would still be valid if the dissociation fractions for the jet and residual-hydrogen particles were the same (i.e., if K was independent of T), as we came to expect must be the case.

It was apparent that the H-atom reflection probabilities from the walls of our scattering chamber (and the apparatus inside) must be very close to unity. Otherwise, H atoms could not survive the large number of wall collisions required (on average) to be present as targets for the beam ions in the region upstream from the ion deflectors. This was obviously in conflict with such calculated reflection-probability values[30] as 0.1. We soon realized, however, that such calculations[31] apply only to "clean" surfaces. We should have expected that the layers of H_2O molecules, loosely bound to the walls of unbaked vacuum systems such as ours by their large dipole moments, would invalidate the use of such clean-surface data.[33]

However, the interior surface of the water-cooled shield surrounding the furnace tube itself (see Fig. 1) should be quite clean, the result of being exposed to the intense photon flux from the hot furnace, and the tungsten sputtered from the furnace tube by the energetic (up to 1 keV) heating electrons.[21] Thus, H-atom recombination[31] should occur on the interior surface of this shield, which intercepts about 75–80 % of the total gas flow from the furnace. In fact, if only this fraction of the H atoms leaving the furnace could recombine, we might expect the dissociation fraction for the hydrogen particles in the furnace chamber (and, therefore, in the jet) to be some 20–25 % of that in the target beam. This is certainly in good agreement with the measured value (22%) found[32] for the residual hydrogen present in the scattering chamber.

While such agreement supported our contention that the dissociation of the jet and residual-hydrogen particles was already established before they emerged from the furnace chamber, we did perform a lengthy series of diagnostic studies to confirm this hypothesis. For example, some data were taken with the first beam-skimming aperture (see Fig. 1) removed. This significantly altered the properties of the jet relative to the target beam and, consequently, such measured signals as $S_F(T)$ and $S_f(T)$. However, the desired signal ratio $S_t(T)/S_t(T_0)$ needed

to find σ_a/σ_m via Eq. (3) in this modified configuration (for 0.5-keV H^+ impact on H and H_2 at $T=2400$ K) was found to be $5.49\pm6.9\%$, in excellent agreement with our final "best value" of $5.55\pm5.6\%$.

Another approach taken was to mathematically simulate various expected H-atom signals as functions of furnace temperature using arbitrarily assigned values of the jet dissociation fraction. The departure of these signals from those measured allowed us to place quantitative limits on this dissociation fraction. It is not possible in this space to review these results[22] in a meaningful way, so we simply state our conclusion. That is, as far as we could tell, the dissociation fraction of the particles in the jet was identical to that measured for the residual hydrogen in the scattering chamber, but could not exceed 1.2 times this value.[32]

As final evidence for this conclusion, we show in Fig. 5(b) the $S_t(T)$ data obtained using Eq. (9), and the measured $S_F(T)$ and $S_f(T)$ signals shown in Fig. 5(a). The K value indicated on the graph was typical of such results for an ac ion beam at 0.5-keV H^+ energy.[26] The data points plotted are compared with a calculated signal predicted from Eq. (2), using the relative effective target-beam densities shown in Fig. 3, and the σ_a/σ_m ratio indicated (which is within about 1% of the average of all our measurements). Such good agreement between measured and predicted signals would be unlikely, if the properties of the jet had not been properly accounted for.

While diagnostic studies such as discussed above were made at various ion energies between 2.0 and 0.125 keV, it was generally not necessary to acquire such detailed data at all furnace temperatures. Normally, measurements of the H-atom signals described by Eqs. (4)–(7) were made only at room temperature and near $T=2400$ K (including measurements of the signals from ion impact on the background-gas particles under both hot- and cold-furnace conditions). Equation (10) was used to determine values of the parameter K from these measured signals, and Eq. (9) was used at both (T) and (T_0) to find $S_t(T)$ and $S_t(T_0)$, respectively. Typically, about five such measurements were made at each projectile energy, and statistical scatter was assessed at twice the goodness of the mean (or about 90% CL). These data were applied via Eq. (3) to find σ_a/σ_m, or $S_t(T_0)$ applied via Eq. (1) to find the ion-energy dependence of σ_m, using the computed effective-target-beam densities as required.

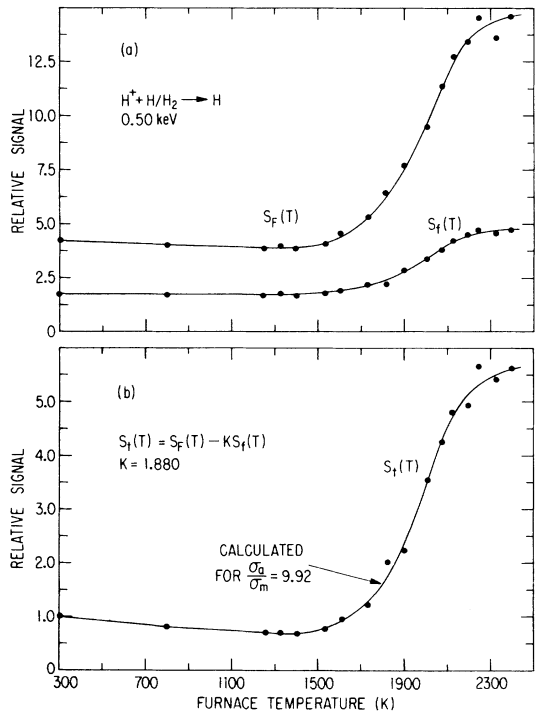

FIG. 5. Relative values of H-atom signals $S_F(T)$, $S_f(T)$, and $S_t(T)$ vs furnace temperature.

IV. FINAL CROSS-SECTION DATA AND DISCUSSION

Using the techniques described in Secs. II and III, it was possible to measure the relative values of σ_{10} and σ_{-10} for H^+ and H^- impact on both H and H_2 targets. It was not possible, however, to measure (to the desired accuracy) any cross section absolutely. It was therefore necessary to choose a value of some cross section at some ion energy to serve as a calibration standard.

After careful scrutiny of all the available data, we adopted the value $\sigma_{10}=6.95\times10^{-16}$ cm^2 for H^+ impact on H_2 at 2.0-keV H^+ energy as our standard. This value was basically obtained from the data of McClure,[6] by careful extrapolation between his reported results at 1.92 and 2.41-keV H^+ energy. Also, for H^+ energies between about 1.5 and 5.0 keV, the data of McClure[6] lie very close (usually within $\pm3\%$) to the average of numerous other results, including data from Stedeford and Hasted,[11] Stier and Barnett,[34] Curran *et al.*,[35] Hollricher,[36] and Williams and Dunbar.[37] We here assign an uncertainty of $\pm9.0\%$ to this standard. This is probably overly conservative, in view of the $\pm4\%$ uncertainty cited by McClure,[6] and his good agreement with the (averaged) data noted above. It is, however, in keeping with our citing all uncertainties at the 90% CL or higher.

The σ_m, σ_a/σ_m, and σ_a results of our measurements for H^+ impact on H and H_2 and their uncertainties are presented in Table I. The uncertainties in σ_m were obtained from the individual (90% CL) uncertainties found in determining the relative values of $S_t(T_0)$, γ^-, and $N_{tm}(T_0)$ as functions of H^+ energy, and the $\pm9.0\%$ uncertainty assigned to the cross-section standard at 2-keV H^+ energy. These uncertainties were judged to be uncorrelated and were thus combined in quadrature. The uncertainties in σ_a/σ_m were found in the same way from the uncertainties in the hot- and cold-furnace H-atom-signal and effective target-beam-density ratios. Values of σ_a were obtained directly from the products of σ_m and σ_a/σ_m, whose uncertainties were combined in quadrature to give those for σ_a. Our data are compared with other work in Fig. 6 (and can be easily identified by their plotted uncertainty flags).

TABLE I. Electron-capture cross sections for H^+ impact on H and H_2.

E (keV)	σ_m (10^{-16} cm^2)	σ_a/σ_m	σ_a (10^{-16} cm^2)
2.000	6.95 ±9%	2.00±15%	13.9±17%
1.414	5.86 ±13%	2.58±11%	15.1±17%
1.000	4.43 ±14%	3.68±11%	16.3±18%
0.707	3.05 ±13%	5.87±10%	17.9±17%
0.500	1.92 ±14%	9.82±10%	18.9±17%
0.354	1.19 ±14%	17.5 ±11%	20.8±17%
0.250	0.790±14%	27.7 ±12%	21.9±19%
0.177	0.537±21%	37.6 ±16%	20.2±26%
0.125	0.423±17%	58.0 ±14%	24.5±22%
0.088	0.345±16%	83.2 ±12%	28.7±20%
0.063	0.334±26%	79.2 ±14%	26.5±28%

For the case of H_2 targets, Fig. 6 shows that there is reasonable agreement among the data plotted[38] for H^+ energies above 1 keV (justifying our cross-section standard choice discussed above). For H^+ energies below 1 keV, our results and those of Koopman,[14] shown as the dotted-line curve, are hardly distinguishable. These two sets of data also lie close to the average (over the scatter) of the other low-H^+-energy results, confirming the apparent "leveling off" of σ_{10} at the lower H^+ energies.[39] This feature conflicts with such crude semiclassical predictions as made by Rapp and Francis,[40] for example, which suggest σ_{10} should scale as E^2 at low H^+ energy E. This structure may result from the opening of new interaction channels caused by the transient existence of H_3^+ during the collisions.

For H-atom targets our data are in good agreement with those reported by McClure[6] above 2-keV H^+ energy, and those obtained by Newman *et al.*[7] for H^+ energies below 0.3 keV. The older results of Fite *et al.*[5] are somewhat larger in magnitude, but much of this discrepancy can be accounted for by their use of a larger σ_m value (by about 10%) as a reference for their σ_a/σ_m measurements. The dashed-line curve shown in Fig. 6 could easily be mistaken for a "best fit" to our data, but is actually the theoretical prediction of Dalgarno and Yadav.[3] As can be seen, we could equally well have used these theoretical results as our cross-section standard.

Our corresponding results for σ_{-10} are presented in Table II and compared with other data in Fig. 7. The value of σ_m at 2-keV H^- energy was established here by careful measurement of σ_{-10}/σ_{10} on several occasions

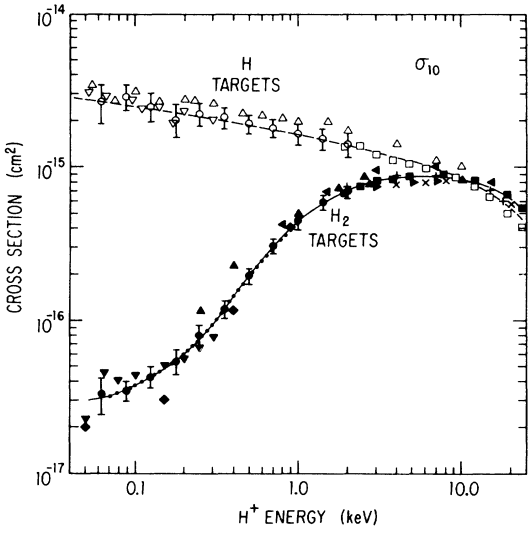

FIG. 6. Electron-capture cross sections for H^+ impact on H and H_2. The measured data are from ●, ○, present results; △, Fite *et al.* (Ref. 5); ■, □, McClure (Ref. 6); ▽, Newman *et al.* (Ref. 7); ▲, Stedford and Hasted (Ref. 11); ◆, Gustafson and Lindholm (Ref. 12); ▼, Cramer (Ref. 13); ×, Stier and Barnett (Ref. 34); ▶, Curran *et al.* (Ref. 35); ◀, Hollricher (Ref. 36); and +, Williams and Dunbar (Ref. 37). The dotted-line curve is from the curve of Koopman (Ref. 14). The dashed-line curve is the theory of Dalgarno and Yadav (Ref. 3).

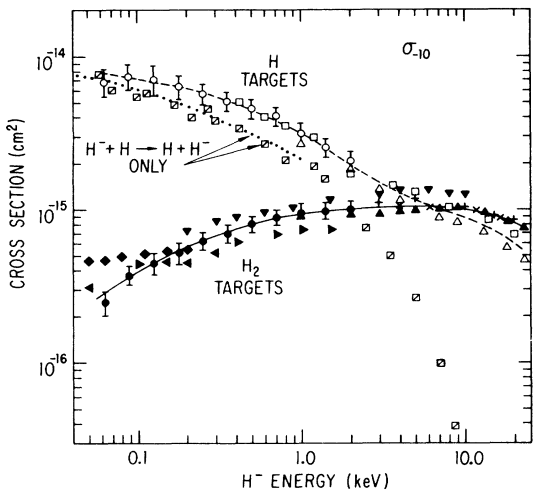

FIG. 7. Electron-loss cross sections for H^- impact on H and H_2. The measured data are from ●, ○, present results; ▲, △, Geddes *et al.* (Ref. 8); ◪, □, Hummer *et al.* (Ref. 9); ▶, Hasted and Smith (Ref. 15); ◀, Muschlitz *et al.* (Ref. 16); ▼, Risley and Geballe (Ref. 17); ◆, Huq *et al.* (Ref. 18); ×, Stier and Barnett (Ref. 34); and +, Simpson and Gilbody (Ref. 41). The dotted line curve is the theory of Dalgarno and McDowell (Ref. 10).

TABLE II. Electron-loss cross sections for H^- impact on H and H_2.

E (keV)	σ_m (10^{-16} cm^2)	σ_a/σ_m	σ_a (10^{-16} cm^2)
2.000	9.99±10%	2.08±11%	20.7±15%
1.414	9.83±14%	2.56±10%	25.2±17%
1.000	9.54±16%	3.27±11%	31.2±19%
0.707	8.89±15%	4.55±11%	40.5±19%
0.500	8.02±15%	5.64±11%	45.2±18%
0.354	6.94±15%	7.31±10%	50.7±18%
0.250	6.20±16%	9.26±10%	57.4±19%
0.177	5.16±18%	12.2 ±11%	62.9±21%
0.125	4.46±17%	15.9 ±18%	70.9±25%
0.088	3.70±19%	20.3 ±14%	75.0±24%
0.063	2.48±24%	27.4 ±17%	68.1±29%

(yielding 1.437±4.9%), and using the same σ_{10} standard discussed above.

For H_2 targets, our measured σ_m values are in good agreement with those of Geddes *et al.*[8] for H^- energies in the 1–2-keV range, and merge smoothly at higher H^- energies onto the data of Stier and Barnett,[34] Simpson and Gilbody,[41] and Williams.[42] (The results of Williams[42] were not plotted[38] in Fig. 7, because they lie so close to those shown for Geddes *et al.*[8]) For H^- energies down to near 0.2 keV, our data lie above those of Hasted and Smith[15] and Muschlitz *et al.*,[16] but below those of Risley and Geballe.[17] However, all these results assign a generally similar H^--energy dependence to σ_{-10}, and all agree with the present data to within mutual uncertainties.

Unfortunately, the situation is less satisfactory at the very low H^- energies, where our results and those of Muschlitz *et al.*[16] and Huq *et al.*[18] seem to diverge when decreasing H^- energy. (Our data could be reasonably extrapolated to 1.5×10^{-16} cm^2 at 0.025-keV H^- energy, the value found by Hasted and Smith.[15] This value, however, is almost a factor of 3 below that of Huq *et al.*[18]) Such comparisons, however, must be made with care. Of the results shown in Fig. 7 for H^- energies below 1.0 keV, only our experiment actually measured σ_{-10}. The others measured $\sigma_{-10}+2\sigma_{-11}$, the latter being the cross section for two-electron loss by H^-, and therefore represent only upper limits on σ_{-10}. Both Geddes *et al.*[8] and Williams[42] have found that σ_{-11} is much smaller than σ_{-10} at high H^- energies, but again the existence of the collisionally transient H_3^- complex at these very low H^- energies could alter the nature of the interaction here, although so large an effect seems unlikely.

For the case of H-atom targets, our σ_{-10}, that of Geddes *et al.*[8] above 1.0-keV H^- energy, and that of Hummer *et al.*[9] above 0.4-keV H^- energy, are all reasonably close. The results of Hummer *et al.*[9] for the $H^-+H\rightarrow H+H^-$ electron-capture component of σ_{-10} also agree well with the theory of Dalgarno and McDowell.[10] Comparison of all these data indicates that the $H^-+H\rightarrow H+H+e^-$ electron-stripping component of σ_{-10} remains quite large down to H^- energies well below 0.4 keV, as suspected by Hummer *et al.*[9] Note also that there is an indication that our data point at 0.063-keV H^- energy may be somewhat low. This could indicate that our σ_m value may also be low here (if our measured σ_a/σ_m is accepted), reducing at least slightly the apparent discrepancy in the σ_m data discussed above.

In summary, the σ_{10} and σ_{-10} data reported here for H^+ and H^- impact on H atoms are in very satisfactory agreement with other results, the agreement with theory[3,10] being particularly pleasing. With the exception of σ_{-10} at the very low H^- energies, the data obtained for H_2 targets also clarify the available information about these collisions. Finally, we conclude that the basic experimental techniques described here are adequate to allow the more difficult measurements noted in Sec. I to be made, beginning with our study of H + H collisions to be described in paper II.

ACKNOWLEDGMENTS

The authors express their thanks to H. Neumann and R. C. Amme for their contributions to these measurements. This work has been supported by the Aeronomy Program, Division of Atmospheric Sciences, National Science Foundation, the Boettcher Foundation, and the Donald H. Menzel Endowment Fund at the University of Denver.

*Present address: Department of Physics and Astronomy, University of Nebraska, Lincoln, NE 68588.

[1]M. W. Gealy and B. Van Zyl, following paper, Phys. Rev. A **36**, 3100 (1987).
[2]J. D. Jackson and H. Schiff, Phys. Rev. **89**, 359 (1953).
[3]A. Dalgarno and H. N. Yadav, Proc. Phys. Soc. (London), Sect. A **66**, 173 (1953).
[4]R. Shakeshaft, Phys. Rev. A **18**, 1930 (1978).
[5]W. L. Fite, R. T. Brackmann, and W. R. Snow, Phys. Rev. **112**, 1161 (1958); W. L. Fite, R. F. Stebbings, D. G. Hummer, and R. T. Brackmann, Phys. Rev. **119**, 663 (1960); W. L. Fite, A. C. H. Smith, and R. F. Stebbings, Proc. R. Soc.

(London), Sect. A **268**, 527 (1962).
[6]G. W. McClure, Phys. Rev. **148**, 47 (1966).
[7]J. H. Newman, J. D. Cogan, D. L. Ziegler, D. E. Nitz, R. D. Rundel, K. A. Smith, and R. F. Stebbings, Phys. Rev. A **25**, 2976 (1982).
[8]J. Geddes, J. Hill, M. B. Shah, T. V. Goffe, and H. B. Gilbody, J. Phys. B **13**, 319 (1980).
[9]D. G. Hummer, R. F. Stebbings, W. L. Fite, and L. M. Branscomb, Phys. Rev. **119**, 668 (1960).
[10]A. Dalgarno and M. R. C. McDowell, Proc. Phys. Soc. (London), Sect. A **69**, 615 (1956).
[11]J. B. H. Stedeford and J. B. Hasted, Proc. R. Soc. (London), Sect. A **227**, 466 (1955).
[12]E. Gustafson and E. Lindholm, Ark. Fys. **18**, 219 (1960).
[13]W. H. Cramer, J. Chem. Phys. **35**, 836 (1961).
[14]D. W. Koopman, Phys. Rev. **154**, 79 (1967).
[15]J. B. Hasted and R. A. Smith, Proc. R. Soc. (London), Sect. A **235**, 349 (1956).
[16]E. E. Muschlitz, Jr., T. L. Bailey, and J. H. Simons, J. Chem. Phys. **24**, 1202 (1956); **26**, 711 (1957).
[17]J. S. Risley and R. Geballe, Phys. Rev. A **9**, 2485 (1974).
[18]M. S. Huq, L. D. Doverspike, and R. L. Champion, Phys. Rev. A **27**, 2831 (1983).
[19]B. Van Zyl, N. G. Utterback, and R. C. Amme, Rev. Sci. Instrum. **47**, 814 (1976).
[20]An important feature not shown in Fig. 1 is the numerous openings in the water-cooled shield between the reservoir and last filament. These openings allowed most gas to flow from the shield into the furnace vacuum chamber without flooding into the region near the differential-pumping and beam-skimming apertures.
[21]B. Van Zyl and M. W. Gealy, Rev. Sci. Instrum. **57**, 359 (1986).
[22]M. W. Gealy, Ph.D. thesis, University of Denver, 1986.
[23]J. A. Ray, C. F. Barnett, and B. Van Zyl, J. Appl. Phys. **50**, 6516 (1979).
[24]B. Van Zyl, M. W. Gealy, and H. Neumann, Phys. Rev. A **28**, 2141 (1983).
[25]To overcome this problem, it was necessary to measure σ_{10} for $H^+ + H_2$ collisions using target-beam densities up to an order of magnitude larger than normal. These could be obtained by using correspondingly higher furnace-reservoir pressures, as long as the furnace was kept at room temperature.
[26]These ion paths and their ratio were somewhat different when the ion beams were operated in ac modes beyond the auxiliary ion collector discussed in Sec. II. This results from the need to add 3.3 cm (equivalent distance at 50% beam intensity) to each of these ion paths, so their ratio is reduced to 1.35 from 1.46.
[27]We introduced H_2 directly into the scattering chamber and measured deflectors off and on signal ratios, giving $1.457 \pm 0.7\%$. The good agreement of this value with the 1.46 computed from component separations in the system strongly supports this assertion.
[28]In fact, most of these jet particles impacted the front surface of the quadrupole chamber, whose entrance aperture was only 0.9 cm tall to limit the backflow of gas from this chamber. Crude estimates suggested that perhaps as much as $\frac{2}{3}$ of what we here call the jet was therefore actually the result of the initial jet particles bouncing around between the various surfaces (see Fig. 2) surrounding the somewhat-enclosed interaction region.
[29]We did not experimentally investigate this conclusion for the case of $H^+ + H$ collisions. However, the energy-resonant nature of this reaction and its attendant large electron-capture cross section together with the smaller target mass makes it highly unlikely that more angular scattering would occur here.
[30]M. I. Baskes, J. Nucl. Mat. **128/129**, 676 (1984).
[31]M. I. Baskes (private communication). Such H atoms are presumably chemically bound to the surface, over which they migrate until encountering other H atoms. Recombination can then occur, and the resulting H_2, being unbound, are free to leave the surface.
[32]Such increases in $S_f(T)$ with furnace temperature became much more pronounced at lower H^+ energies, where the σ_a/σ_m ratio is much larger. Using such data, we were able to show that the dissociation fraction of the residual hydrogen in the scattering chamber was about $22\% \pm 3\%$ of that in the target beam for $T > 1500$ K.
[33]In fact, it is difficult to postulate any mechanism which would allow thermal-energy H atoms to "stick" on such an H_2O-covered surface. H_3O is not stable, and chemical processes leading to H-atom recombination are endothermic. Thus, in retrospect, a near unit reflection probability seems reasonable.
[34]P. M. Stier and C. F. Barnett, Phys. Rev. **103**, 896 (1956).
[35]R. Curran, T. M. Donahue, and W. H. Kasner, Phys. Rev. **114**, 490 (1959).
[36]D. Hollricher, Z. Phys. **187**, 41 (1965).
[37]J. F. Williams and D. N. F. Dunbar, Phys. Rev. **149**, 62 (1966).
[38]It was not possible to plot all the available data for this reaction, or even more than a few representative data points from each of the references cited.
[39]Such a leveling off of σ_{10} could have resulted from an impurity species with a much larger σ_{10} present in the H_2-gas sample. We used two ultrahigh-purity samples to show this was not the case.
[40]D. Rapp and W. E. Francis, J. Chem. Phys. **37**, 2631 (1962).
[41]F. R. Simpson and H. B. Gilbody, J. Phys. B **5**, 1959 (1972).
[42]J. F. Williams, Phys. Rev. **154**, 9 (1967).